Available online at www.sciencedirect.com
SCIENCE DIRECT®
Journal of Power Sources 126 (2004) 125–133
JOURNAL OF POWER SOURCES
www.elsevier.com/locate/jpowsour

Visualization of particle distribution in composite polymer electrolyte systems

S. Zhang, Jim Y. Lee*, L. Hong

Department of Chemical & Environmental Engineering, National University of Singapore, 10 Kent Ridge Crescent, Singapore 119260, Singapore

Received 4 July 2003; accepted 13 August 2003

Abstract

A simple visualization method is developed to enable the imaging of the distribution and agglomeration of ceramic fillers in composite polymer electrolytes by scanning electron microscopy (SEM). Solvent-free composite electrolytes based on poly(ethylene oxide) (PEO), $LiBF_4$ and SiO_2 particles are used as examples. The SiO_2 particles are stained by a heavy element (Pb) to enhance the imaging contrast between the particles and their surroundings. Modified SiO_2 from a silanization reaction where most of the surface OH groups has been replaced by Si-phenyl groups is also used to reduce the Lewis acid–base interactions between the ceramic fillers, the polymer and the Li salt. Although nearly the same particle size and particle distribution are found for SiO_2 and modified SiO_2 in PEO, the two composite electrolyte systems exhibit remarkably different electrochemical transport properties. The difference can, therefore, be unambiguously attributed to the benefit of Lewis acid–base interactions.

Keywords: Poly(ethylene) oxide; Polymer electrolyte; Ceramic filler; Morphology; Surface groups; Lithium batteries

1. Introduction

Polymer electrolytes are solid solutions of organic or inorganic salts in polymers where the segmental motion of the polymer chains is the primary driving force for ion conduction [1,2]. Among the polymer electrolytes of practical interest, the poly(ethylene oxide)-lithium (PEO-Li) system is most promising for applications in rechargeable lithium batteries. PEO excels as a polymer host because of its commercial availability, its high solvating power for the lithium ions and its compatibility with the lithium electrode. On the other hand, the ionic conductivity of PEO-based electrolytes at room temperature ($\sigma < 10^{-7}$ S cm^{-1} at 25 °C) is too low to be useful [1,2]. The ionic conductivity has been enhanced by various means [3–18], but one of the most promising methods is to add fine ceramic fillers such as TiO_2, SiO_2, Al_2O_3, ZrO_2 to the polymer [19–27]. The enhancement is believed to be due to the combination of: (i) the amorphitization of PEO; (ii) Lewis acid–base interactions between the ceramic fillers, the PEO chains, and the counter ions that result in greater ionization of the lithium salt in PEO and the faster transport of lithium ions through the electrolyte [22,28–30]. The effects of particle size and the nature of the ceramic filler on the properties of the composite electrolytes have also been reported [24,25,31–33].

Despite the above studies, there is no simple method for visualizing the particle morphology and the state of particle dispersion in the polymer electrolytes. The use of compositional imaging by backscattered electrons in a scanning electron microscope [34] has only met with limited success. In this work, SiO_2 particles have been stained by lead to enhance the imaging contrast between the ceramic particles and their surroundings when examined by scanning electron microscopy (SEM). Two types of SiO_2 particles have been used, namely, commercial SiO_2 particles and SiO_2 particles which have been modified to remove most of the surface OH groups. The modified SiO_2 is expected to replicate almost all aspects of the SiO_2 functionalities except Lewis acid–base interactions. The particle size is not altered by the surface modification and if the Pb-staining technique indicates nearly similar particle distribution in PEO, then the difference in electrochemical transport properties between the two composite polymer electrolyte systems can only arise from Lewis acid–base interactions. The experimental results can then be used to deduce the relative importance of the passive (fillers as polymer amorphitizers, strength enhancers, and impurity getters) and electronic (Lewis acid–base interactions) effects of SiO_2 addition.

* Corresponding author. Tel.: +65-6874-2899; fax: +65-6779-1936.
E-mail address: cheleejy@nus.edu.sg (J.Y. Lee).

0378-7753/$ – see front matter © 2003 Elsevier B.V. All rights reserved.
doi:10.1016/j.jpowsour.2003.08.011

2. Experimental

2.1. Materials

Poly(ethylene oxide) (PEO, MW = 900,000), high surface area SiO_2 ($390\,m^2\,g^{-1}$, particle size = 7 nm), triethylamine (Et_3N), $LiBF_4$, $Pb(NO_3)_2$, tetrahydrofuran (THF), and $NaBH_4$ were supplied by Aldrich and used without further purification. Acetonitrile (gradient grade) from Merck was used as the solvent in casting polymer electrolyte membranes. Toluene (99.9%) was supplied by Baker. Phenyltrimethoxysilane (PMOS, 97%) from Fluka was used as the silanization agent to remove the surface OH groups on SiO_2.

2.2. Modification of SiO_2

The OH groups on the SiO_2 surface are reactive in silanization reactions and can be removed. In a typical experiment, 500 mg of SiO_2 and 1 ml PMOS were dispersed in 50 ml of toluene together with 0.15 ml of Et_3N added as catalyst. The resulting mixture was stirred at room temperature under an argon atmosphere for 24 h. The SiO_2 was recovered as a moist slurry after centrifuging the mixture at 15 000 rpm for 15 min. The slurry was washed with THF, re-dispersed in THF and re-centrifuged several times in order to remove excess PMOS. The slurry was dried to a powder in vacuum at 60 °C for 72 h, and stored in a M Braun glove-box in which the moisture and oxygen contents were each below 1 ppm. Untreated SiO_2 was also dried in vacuum and stored in the glove-box for comparative studies.

2.3. Characterization of modified SiO_2 powders

The modified SiO_2 particles were characterized by Fourier-transform infrared spectroscopy (FT-IR), thermogravimetry analysis (TGA) and element analysis. FT-IR spectra were obtained on a Bio-Rad FTS 135 spectrometer. Each spectrum was the result of 16 scans in the range 400 to 4000 cm^{-1} sampled at 8 cm^{-1} resolution. Thermogravimetry analysis of samples was carried out using a TA Instruments TGA 2090 analyzer with temperature ramping from room temperature to 800 °C at a rate of 10 °C per min. A PE 2400 Series II CHN analyzer from Perkin-Elmer was used to determine the carbon and hydrogen contents in the samples.

2.4. Preparation of composite electrolyte membranes

The following procedures were carried out in the M Braun recirculating argon glove-box. Calculated amounts of PEO, $LiBF_4$ and SiO_2 (or modified SiO_2) were dissolved and dispersed in acetonitrile at 40 °C and stirred continuously for 12 h to obtain a homogeneous suspension. The molar ratio of EO to Li was fixed at 8:1 for all samples. The solution was cast on to a flat polytetrafluoroethylene (PTFE) petri dish and covered. The solvent was allowed to evaporate slowly and the resulting membrane was dried at 40 °C for 2 to 3 days until a constant weight was reached. Homogeneous and mechanically stable membranes with thickness in the range 60 to 80 μm could be obtained this way.

2.5. Visualization of SiO_2 particles in polymer electrolyte membranes

In this work, an attempt is made to visualize the size, the morphology, and the distribution of SiO_2 particles in the polymer electrolyte by staining the particles with Pb, a heavy element rich in electrons, to interact with the incident analytical electron beam to enhance the imaging contrast between SiO_2 and the polymer. The following staining procedure was used. Five hundred milligrams of SiO_2 and 39.96 mg $Pb(NO_3)_2$ were ultrasonically dispersed in 20 ml distilled water for several hours to obtain a homogeneous suspension. Excess $NaBH_4$ solution was slowly introduced to the mixture to reduce Pb(II) to Pb(0). The precipitated lead was preferentially adsorbed by the suspended ceramic particles because of their large surface area. The loading of lead in SiO_2 according to EDX measurements was 4 wt.%. The lead-stained SiO_2 was recovered, repeatedly washed by water and then by THF, dried in vacuum for 72 h, and finally transfer to the M Braun glove-box. A small amount of the homogeneous composite electrolyte solution containing the lead-stained SiO_2 particles was dropped on to a SEM or TEM copper grid. The grid was attached to a spin-coating machine (Cost Effective Equipment- Model 100) and spun at 2000 to 2500 rpm for 30 to 60 s to obtain thin films. For SEM examination, the surface of the thin film was coated with a layer of platinum to reduce the electrostatic charging of non-conducting samples. Before TEM imaging, a thin film of amorphous carbon was deposited on the sample for further protection and stabilization during exposure to the electron beam exposure. A JSM-5600 LV scanning electron microscope (SEM) operating at 15 kV, and a JEM-2010 transmission electron microscope operating at 200 kV were used for SEM and TEM characterizations of morphology and microstructures.

2.6. Measurements of electrochemical properties

Electrochemical measurements were carried out using blocking SS/composite electrolyte/SS cells (SS = stainless steel). An Eco Chemie PGSTAT 30 potentiostat/galvanostat equipped with a frequency response analyzer module was used to obtain the electrochemical impedance of samples between 30 and 90 °C. Ionic conductivity was calculated from the impedance response using a widely-accepted equivalent circuit model and extracting the bulk resistance of the electrolyte from the high frequency response [35–37].

For the measurement of Li^+ transference numbers, lithium metal was used for both electrodes to constitute a symmetric test cell with the configuration of Li|electrolyte|Li.

The electrochemical impedance was first measured before a d.c. bias of 10 mV was applied to the cell. The current response of the cell was monitored over time until a steady-state was reached. Another measurement of the cell impedance was them made to complete the procedure. The data were then analyzed by the method reported in [38].

3. Results and discussion

3.1. Characterization of modified SiO_2

Ceramic particles, such as SiO_2, Al_2O_3, and TiO_2, have been used as polymer fillers in order to obtain composite materials with enhanced properties (mechanical, thermal, electrical, and magnetic). It has been shown [39,40] that the surface modification of these particles can improve the compatibility and adhesion between the ceramic particles and the polymer matrix.

The surface OH groups of commercial SiO_2 can be removed by the following silanization reaction:

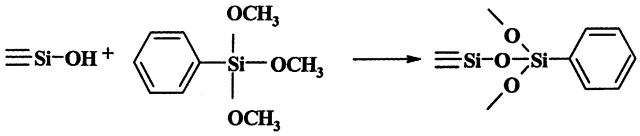

FT-IR provided the evidence of successful displacement of the surface OH groups on SiO_2. The transmission IR spectra of pristine SiO_2, modified SiO_2 and PMOS in the wavenumber range 500 to 4000 cm^{-1} are shown in Fig. 1. The strong infrared absorption broad band with an absorption maximum at 3435.92 cm^{-1} was used to fingerprint the presence of OH groups on the silica surface. Absorption in this spectral region is greatly reduced after the PMOS modification. In addition, peaks began to appear at 1431.99 (stretching vibration of Si-phenyl), 741.78, and 698.32 cm^{-1} (out-of-plane C–H vibrations of the benzene ring) which correspond well with the Si-phenyl vibration of PMOS [41]. The sharp decrease in the OH intensity after the PMOS modification can be attributed to the reactions between the OH groups of SiO_2 and PMOS. It is unlikely that all the OCH_3 groups have reacted because there is still absorption at 2944.8 and 2844.5 cm^{-1} which is generally associated with the asymmetric and symmetric CH stretching of Si-OCH_3 [42].

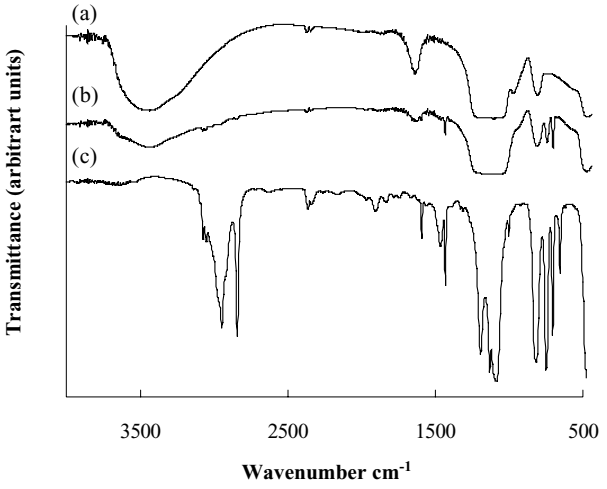

Fig. 1. FT-IR spectra of: (a) pristine SiO_2, (b) PMOS-modified SiO_2, (c) PMOS.

Table 1
Elemental analysis of SiO_2 before and after PMOS modification

	Carbon (wt.%)	Hydrogen (wt.%)
Before modification	0.71	0.71
After modification	17.48	1.71

These observations, when analyzed collectively, confirm that the silanization reaction has successfully displaced most of the OH groups on the SiO_2 surface and replaced them with Si-phenyl groups.

Elemental analysis by CHN and TGA were used to estimate the extent of OH displacement. Based on the results listed in Table 1, the amount of carbon in the untreated SiO_2 is negligible. After silanization, the carbon content in SiO_2 is increased to 17.48 wt.%. The C:H atomic ratio agrees well with the ratio for a phenyl group. The grafting density is estimated to be 18.7 wt.% based on these data. The extent of surface modification can also be deduced from the weight loss after the organic moieties in SiO_2 are completely burnt off at sufficiently high temperatures.

The TGA curves for untreated and modified SiO_2 are shown in Fig. 2(a) and (b), respectively. For the former, the 3% weight loss between 30 and 250 °C can be attributed to the desorption of physi-sorbed water. At higher temperatures, the OH groups on the surface begin to decompose and this accounts for the further weight loss of about 2% in the temperature range 250 to 800 °C. In the case of modified SiO_2, the weight loss between 30 and 250 °C can likewise be attributed to the removal of water. The weight loss

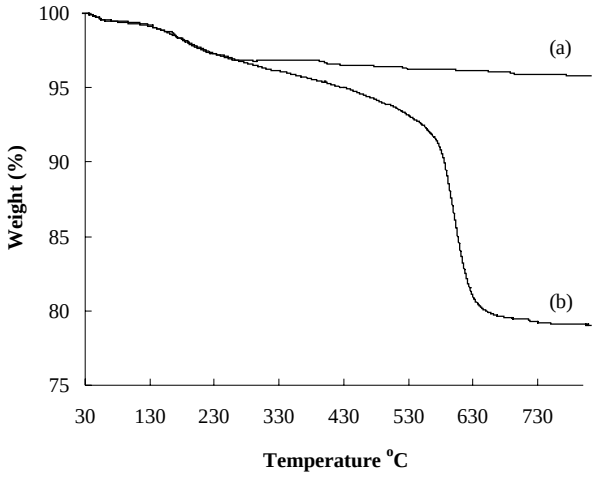

Fig. 2. TGA curves for: (a) pristine, (b) modified SiO_2.

between 250 and 800 °C is significantly higher at 17.7 wt.%, as expected from the thermal decomposition of the organic moieties. This number is fairly close to the elemental analysis results, and indicates that almost all of the surface OH groups have been replaced by Si-phenyl groups.

3.2. Visualization of SiO_2 particles in composite polymer electrolyte membranes

It is well known that PEO-based composite electrolytes have multiphase features when they are prepared by film casting and the compatibility between the polymer and the ceramic fillers has great influence on the properties (thermal, mechanical and optical) of the polymer electrolytes. Normally, three to four phases co-exist in the PEO-based electrolytes, namely, the crystalline PEO phase, the crystalline PEO lithium salt complex phase, the amorphous PEO phase, and the ceramic phase. SEM is often used to assess the compatibility between the various phases through the detection of phase separations and interfaces [34,43–47]. Although the size of the ceramic fillers can be at the nanoscale level (10 nm), it is prudent to investigate whether the ceramic

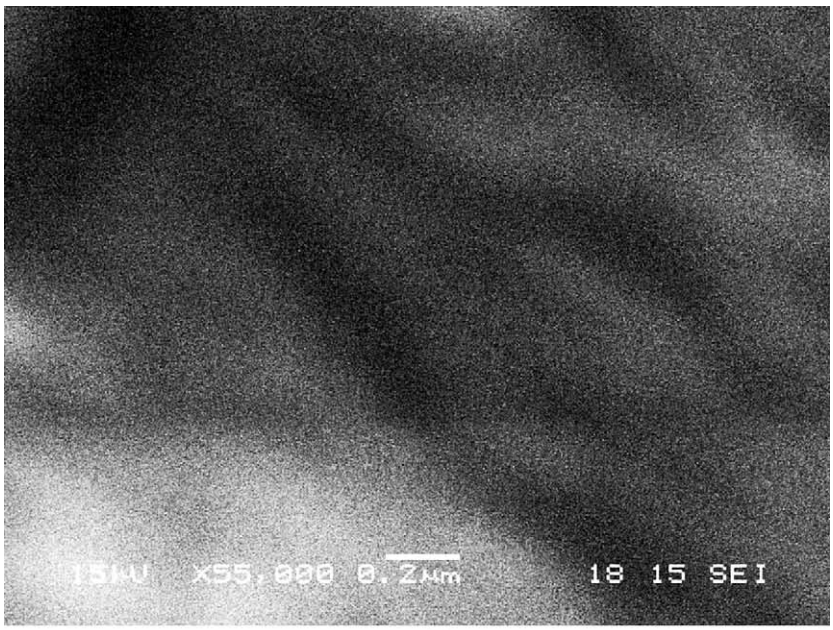

(a)

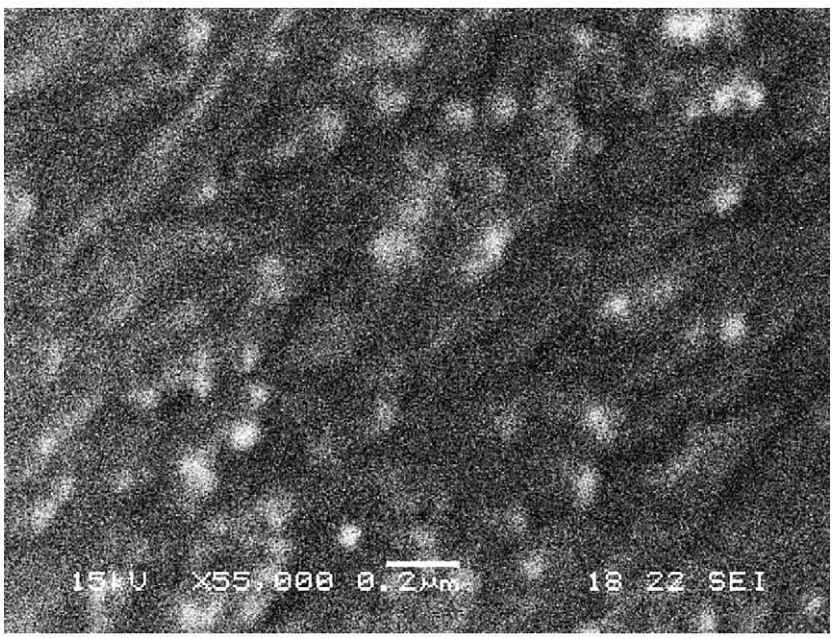

(b)

Fig. 3. Scanning electron micrographs of: (a) PEO with unstained pristine SiO_2, (b) PEO with stained pristine SiO_2, (c) PEO with stained-modified SiO_2.

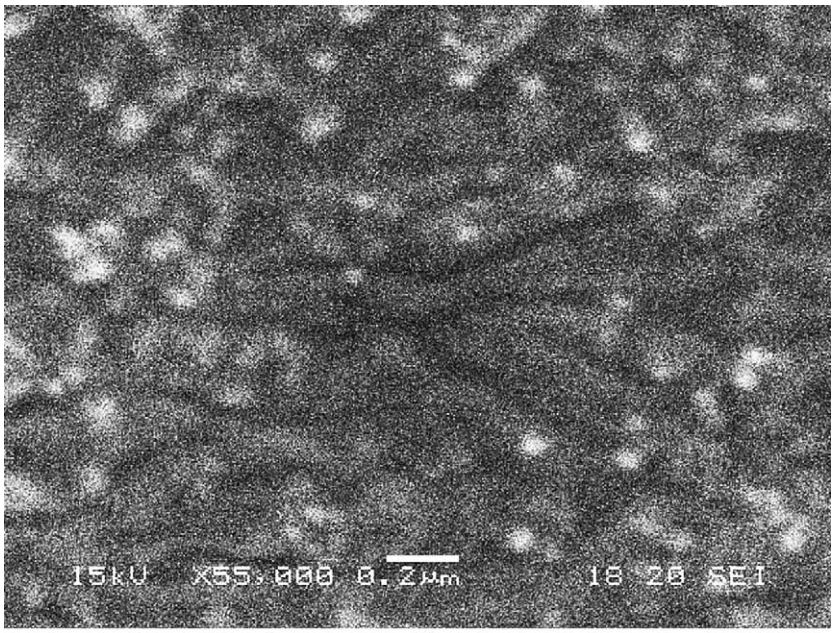

(c)

Fig. 3. (*Continued*).

fillers remain as separate primary particles, or are coagulated by the processes involved in the fabrication of composite polymer electrolytes. There have been very few reports of the size and the morphology of the particles after dispersal in polymer electrolytes.

Generally, the distribution of silica particles in PEO is difficult to visualize by SEM since the two phases do not differ significantly in their ability to radiate secondary electrons upon incidence by the analytical electron beam. In this work, the silica particles are stained by a heavy element (Pb) to increase the number of electrons that can interact with the incident electron beam, and hence will improve the contrast between SiO_2 and the polymer in electron micrographs.

An electron micrograph of unstained SiO_2 in PEO is provided in Fig. 3(a) as the control. The enhancement of the contrast of the micrograph after silica is stained by lead is demonstrated in Fig. 3(b) and (c). It is interesting to note that both the particle size and particle size distribution of untreated and modified SiO_2 in PEO are quite similar. This indicates that the silanization modification has not caused any compatibility issue between the ceramic fillers and the polymer.

Transmission electron microscopy may also be used if the membrane sample is sufficiently thin, to allow the passage of electrons. From the images shown in Fig. 4, it is apparent that the silica particles, with or without modification, have agglomerated to form a loose, open, network structure which is much greater than the 7 nm primary particles.

Lewis acid–base interactions [22,23,26] have been used to rationalize the benefit of ceramic particle addition to polymer electrolytes. It is assumed that the surface groups of the ceramic fillers serve as cross-linking centres for PEO segments and anions, which thereby lowers the tendency for PEO reorganization and promotes structural modifications to the polymer. Facilitated conduction pathways ('effective media' [48,49]) are, therefore, established for lithium ions close to the particle surface. The formation of complexes between the ceramic particles and the electrolyte ionic species also lead to greater lithium salt dissociation. These complexes are unlikely to contribute to the increase in conductivity because of their relatively large mass. The local diffusion within the amorphous polymer matrix is, however, helpful to lithium ion transport, as shown by the higher experimental values of Li^+ transference numbers relative to the ceramic-free electrolytes [26]. The networked particles shown by the TEM images could also be seen as a connected effective medium which further facilitates Li ion transport. The honeycomb-like ceramic particles provide not only provide a larger surface to form numerous ion-ceramic complexes, but also the volume needed to accommodate the PEO that has permeated into the ceramic particles, so as to supply additional conduction channels for the transport of lithium ions [37,50].

The ability to map particle morphology, distribution, and connectivity can add to the understanding of ion transport in a composite electrolyte system. In this work, the addition of modified or unmodified SiO_2 particles has not resulted in any noticeable changes to the physical state of the particles and their distribution in the polymer. Modified silica, however, due to the lack of surface OH groups, is unable to interact chemically with the Li salt or the PEO chains. Its main, and perhaps sole, functionality is to serve as an inert

filler which inhibits crystallization of the polymer. Pristine SiO_2 particles, on the other hand, are chemically active, and may influence salt dissociation and the transport of Li^+ ions through the polymer via Lewis acid–base interactions. The difference in electrochemical properties between the two composite electrolyte systems, if any, can then be attributed to Lewis acid–base interactions since the two systems have nearly the same particle distribution.

3.3. Electrochemical properties of composite polymer electrolytes

For conductivity measurements using two blocking electrodes, the following equation may be used:

$$\sigma = \frac{d}{R_b r^2 \pi} \tag{1}$$

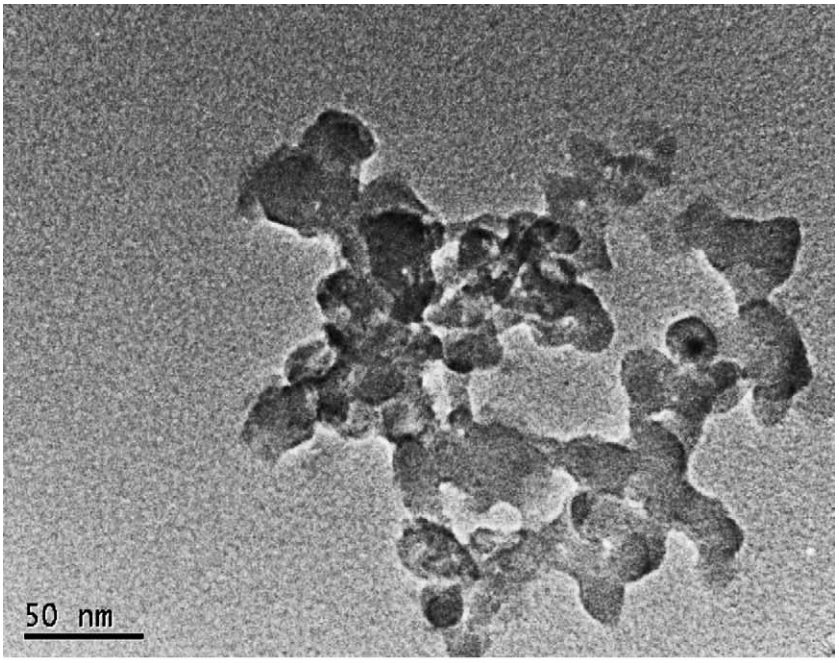

(a)

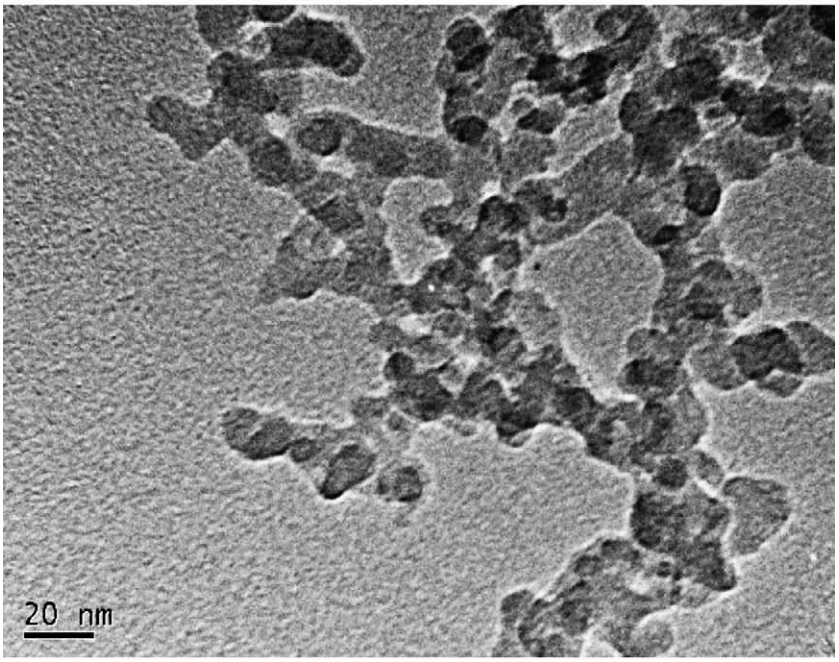

(b)

Fig. 4. Transmission electron micrographs of: (a) PEO with unstained pristine SiO_2, (b) PEO with stained pristine SiO_2, (c) PEO with stained-modified SiO_2.

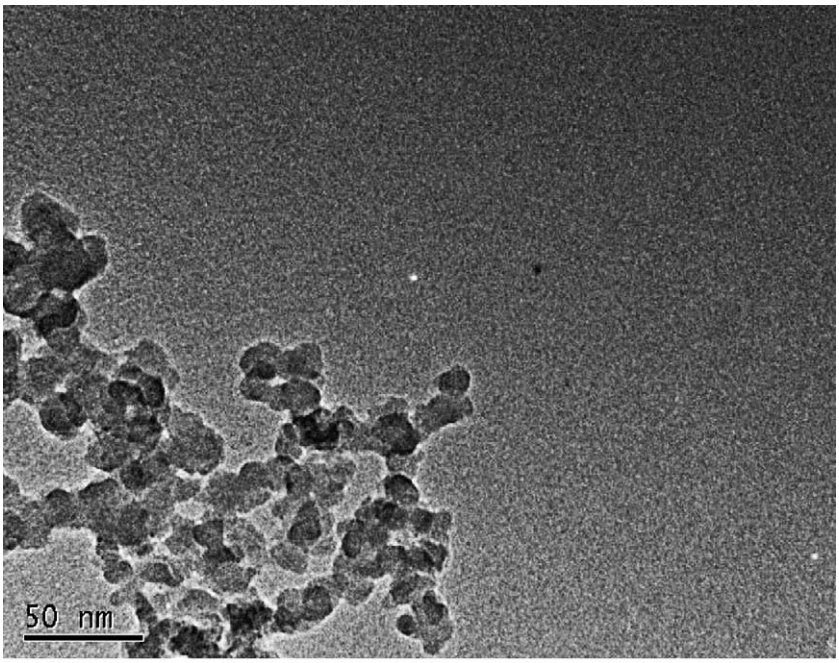

(c)

Fig. 4. (*Continued*).

where, d and r are the thickness and the radius of the sample membrane discs, and R_b is the bulk resistance of the composite electrolyte obtained from complex impedance measurements. It is widely accepted that R_b can be obtained from the intercept on the real axis at the high frequency end of the Nyqisut plot of complex impedance [35,36].

The difference between the temperature dependence of the ionic conductivity of SiO_2 and modified SiO_2 composite polymer electrolytes, as shown in Fig. 5, is within expectation. The increase in ionic conductivity with temperature up to the melting point of PEO is a well-understood phenomenon. For unmodified SiO_2, the interactions between the hydroxyl groups on the silica surface and the ether oxygen atoms of the polymer chains will weaken the co-ordination bonds in the ether O:Li complex, and result in higher Li^+ ion mobility. The same Lewis acid–base interactions also amorphitize the polymer locally around the ceramic particles, which creates more effective conduction pathways for the lithium ions. This can be clearly seen in Fig. 6 at temperatures below the melting point (about

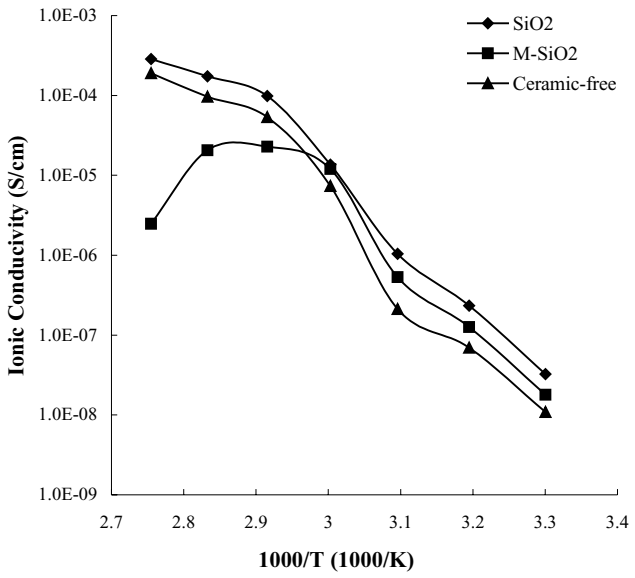

Fig. 5. Temperature-dependence of ionic conductivity.

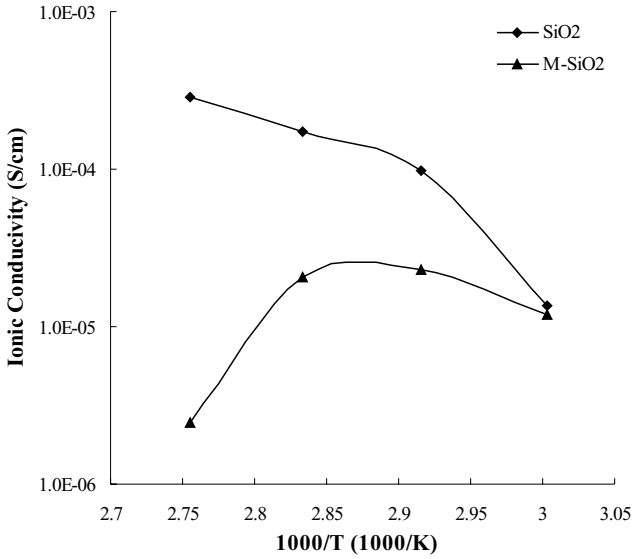

Fig. 6. Temperature-dependence of ionic conductivity between 60 and 90 °C.

68 °C). The polymer is crystalline and hence the conductivity of the ceramic-free polymer electrolyte is lower than that doped with the ceramic particles. In the temperature range 30 to 60 °C the conductivity is higher with unmodified SiO_2 because of the above-mentioned Lewis acid–base interactions. As the density of OH groups is lower in the modified system, the Lewis acid–base interactions are moderated accordingly. This effect is also seen above the PEO melting point, where PEO turns completely amorphous.

The surface OH groups also interact with BF_4^- anions to form hydrogen bonds of the type F∼H–O, which hinder the movement of the anions. For the modified SiO_2 system, the interaction will be reduced because of the lower density of the hydroxyl groups on the surface. Additionally, the phenyl groups introduced by silanization can impose steric hindrance to impede ion transport. This is most easily seen by expanding the high temperature region (60–90 °C) of Fig. 6. While the polymer in this temperature region is completely amorphous, the ionic conductivity in the composite electrolyte is still higher with the SiO_2 addition, which is an indication that the function of SiO_2 is more than the amorphitization of the polymer. On the other hand, there is a decrease in ionic conductivity with temperature when modified SiO_2 is used. This can be explained as follows. The modified SiO_2 particles carry phenyl (-Ph) groups besides OH groups on their surface. As the phenyl group is immiscible with the ethylene oxide unit because of the rather different solubility parameters, there will be phase separation gaps in the vicinities of the modified SiO_2 particles, especially at low temperatures. It is likely that such gaps facilitate, to a certain extent, the migration of Li ions because the PEO segments exposed to the gap can gain a higher degree of freedom. Lithium conductivity is, therefore, boosted through creeping at these boundary segments. With increasing temperature, the gap shrinks steadily because of improved miscibility between the two moieties. At the moment when the gap disappears, the physical entanglement between polymer chains and the bulky-Si (Ph) groups will impede the segmental motions (rotations along a variety of axes) of PEO chains. This interfacial effect will be passed on to the bulk phase of PEO, and hence will drag down the mobility so that the rate of transport of Li ions is severely decreased.

The lithium transference numbers in the SiO_2 and modified SiO_2 systems were also measured to determine the relative contributions of cations and anions to the overall conductivity. The transference numbers were calculated by the method of Evans et al. [38]. The decrease in current from $t = 0$ to the steady-state after the potential of the symmetric test cell was stepped up is the result of two concurrent processes: (i) the growth of passivation layers on the lithium electrode to a limiting thickness; (ii) the establishment of a concentration gradient in the electrolyte which affects the motion of the ions. The following equation is used to calculate the transfer numbers after taking these effects into consideration [38]:

$$T_+ = \frac{I_s(\Delta V - I_0 R_0)}{I_0(\Delta V - I_s R_s)} \quad (2)$$

where, ΔV is the value of the applied d.c. bias (10 mV); R_0 and R_s are the initial and steady-state resistances of the passivation layer obtained from complex impedance measurements; I_0 and I_s are the initial and steady-state currents. The calculated transference numbers are given in Table 2.

Table 2
Li transference numbers for PEO composite electrolytes with pristine and PMOS-modified SiO_2

Sample	Li transference number (T_+)
10%SiO_2-PEO	0.24–0.26
10% modified SiO_2-PEO	0.15–0.20

The Li transference number in the composite electrolyte is an indication of the cationic mobility, which is influenced by the interactions between lithium ions, anions, ether oxygen atoms. and the surface groups of the ceramic particles. The hydrogen bonding between the hydroxyl groups of the ceramic particles and the BF_4^- anions or the ether oxygen atoms of PEO is expected to constrain the movement of BF_4^- anions, even though such interactions might be relatively weak and subtle. The competition between the hydroxyl groups and lithium ions for binding with the ether oxygen atoms of PEO, on the other hand, should promote lithium ion transport [19,26]. These mechanisms, considered collectively, predict a higher Li transference number for systems with high OH densities. For the modified SiO_2 system where the particles contributed primarily to the amorphitization of the polymer without the above-mentioned acid-based interactions, the Li transfer number will be lower even though the ionic conductivity can still be higher than a ceramic-free system.

For the pristine SiO_2-PEO systems, the transference number is calculated to be 0.25. The transference number for modified SiO_2-PEO systems is lower, at 0.18. These numbers fall within the typical range for PEO-based polymer electrolytes ($T_+ = 0.1$ to 0.3 approximately) [51]. The higher transference number of the former, together with the observed higher ionic conductivity, are indications of increased salt dissociation and increased lithium ion mobility in the Polymer which are attributable to the Lewis acid–base interactions between the surface OH groups, the oxygen on the PEO, and BF_4^-. The low Li^+ transference number and low ionic conductivity in the modified SiO_2-PEO system can be categorically assigned to the lack of such interactions.

4. Conclusions

The agglomeration and distribution of ceramic particles in composite electrolytes can be visualized by staining the particles with a heavy element to increase the contrast

between the particles and their surroundings in scanning electron micrograph. This visualization method is used to understand the difference between two composite polymer electrolyte systems based on PEO, $LiBF_4$, and SiO_2 In one of the systems, the OH groups on the SiO_2 filler are replaced by inactive phenyl groups in a silanization reaction with the purpose of reducing the Lewis acid–base interactions between the ceramic particles, the polymer host, and the lithium salt. The two types of SiO_2 particles have similar morphology and dispersion in the polymer, and are expected to amorphitize the polymer to the same extent. Measurements of electrochemical transport properties show that the conductivity of lithium ions is higher in SiO_2-PEO than in modified SiO_2-PEO. The ranking of the transference number follow the same order. While the difference may be unambiguously attributed to the dissimilarity in ceramic surface groups which affects the Lewis acid–base interactions in the composite electrolytes, the decrease in conductivity with temperature for the modified SiO_2-PEO system between 60 and 90 °C can only be speculated as arising from the steric hindrance of the phenyl groups on the silica surface.

References

[1] F.M. Gray, Solid Polymer Electrolytes, VCH, Weinheim, 1991.
[2] M. Gauthier, A. Belanger, B. Kapfer, G. Vassort, M. Armand, in: J.R. MacCallum, C. Vincent (Eds.), Polymer Electrolyte Reviews, vols. 1 and 2, Elsevier, London, 1987/1989.
[3] A. Bouridah, F. Dalard, D. Deroo, H. Cheradame, J.F. Le Nest, Solid State Ionics 15 (1985) 233.
[4] J.F. Le Nest, A. Gandini, H. Cheradame, Br. Polym. J. 20 (1988) 253 (and references therein).
[5] M. Watanabe, A. Suzuki, K. Sanui, N. Ogata, J. Chem. Soc. Jpn. 14 (1986) 428.
[6] D. Benrabah, J.Y. Sanchez, M. Armand, Electrochim. Acta 37 (1992) 1737.
[7] M. Andrei, L. Marchese, A. Roggero, S. Passerini, B. Scrosati, in: B. Scrosati (Ed.), Proceedings of the Second International Symposium on Polymer Electrolytes, Elsevier, London, 1990, p. 107.
[8] X. Peng, H. BA, D. Chen, F. Wang, Electrochim. Acta 37 (1992) 1569.
[9] J.R.M. Giles, F.M. Gray, J.R. Mac Callum, C.A. Vincent, Polymer 28 (1987) 1977.
[10] F.M. Gray, J.R. Mac Callum, C.A. Vincent, J.R.M. Giles, Macromolecules 21 (1988) 392.
[11] M. Armand, M. Gauthier, in: T. Takahashi (Ed.), High Conductivity Solid Ionic Conductors—Recent Trends and Applications, World Scientific, Singapore, 1989, p. 114.
[12] M. Armand, in: Proceedings of the VI International Conference on Solid State Ionics, Garmisch, Germany, 1987, p. 304.
[13] L.A. Dominey, V.R. Koch, T.J. Blakley, Electrochim. Acta 37 (1992) 1551.
[14] B. Scrosati, Application of Electroactive Polymers, Chapman and Hall, London, 1993.
[15] I.E. Kelly, JR. Owen, B.C.H. Steele, J. Electroanal. Chem. 168 (1984) 467.
[16] E. Tsuchida, H. Ohno, K. Sunami, N. Kobayashi, Solid State Ionics 11 (1983) 227.
[17] C. Wang, Q. Liu, Q. Cao, Q. Meng, L. Yang, Solid State Ionics 53–56 (1992) 1106.
[18] R.D.A. Paulkner, A.R. Kulkarni, in: B.V.R. Chowdari, et al. (Eds.), Solid State Ionics—Materials and Applications, World Scientific, Singapore, 1992, p. 549.
[19] F. Croce, G.B. Appetecchi, L. Persi, B. Scrosati, Nature 394 (1998) 456.
[20] F. Croce, R. Curini, A. Martinelli, L. Peris, F. Ronci, B. Scrosati, R. Caminiti, J. Phys. Chem. B 103 (1999) 10632.
[21] B. Scrosati, F. Crose, L. Persi, J. Electrochem. Soc. 147 (5) (2000) 1718.
[22] F. Croce, L. Persi, B. Scrosati, F. Serraino-Fiory, E. Plichta, M.A. Hendrickson, Electrochim. Acta 46 (2001) 2457.
[23] W. Wieczorek, J.R. Stevens, Z. Floijanczyk, Solid State Ionics 85 (1996) 67.
[24] C. Capiglia, P. Mustarelli, E. Quartarone, C. Tomasi, A. Magistris, Solid State Ionics 118 (1999) 73.
[25] H.J. Walls, J. Zhou, J.A. Yerian, P.S. Fedkiw, S.A. Khan, M.K. Stowe, G.L. Baker, J. Power Sources 89 (2000) 156.
[26] S.H. Chung, Y. Wang, L. Persi, F. Croce, S.G. Greenbaum, B. Scrosati, E. Plichta, J. Power Sources 97/98 (2001) 644.
[27] B. Kumar, L.G. Scanlon, Solid State Ionics 124 (1999) 239.
[28] F. Capuano, F. Croce, B. Scrosati, J. Electrochem. Soc. 138 (1991) 1918.
[29] F. Croce, B. Scrosati, J. Power Sources 43/44 (1993) 9.
[30] W. Wieczorek, Z. Florjanczyk, J.R. Stevens, Electrochim. Acta 40 (1995) 2251.
[31] W. Krawiec, L.G. Scanlon, J.P. Fellner, R.A. Vaia, S. Vasudevan, E.P. Giannelis, J. Power Sources 54 (1995) 310.
[32] J. Fan, S.R. Raghavan, X.Y. Yu, S.A. Khan, P.S. Fedkiw, J. Hou, G.L. Baker, Solid State Ionics 111 (1998) 117.
[33] Y. Matsuo, J. Kuwano, Solid State Ionics 79 (1995) 295.
[34] G.-H. Hsiue, W.-J. Kuo, Y.-P. Huang, R.-J. Jeng, Polymer 41 (2000) 2813.
[35] K.M. Abraham, Z. Jiang, B. Carroll, Chem. Mater 9 (1997) 1978–1988.
[36] M. Watanabe, K. Sanui, N. Ogata, T. Kobayashi, Z. Ohtaki, J. Appl. Phys. 57 (1) (1985) 123.
[37] B.A. Boukamp, Solid State Ionics 20 (1986) 31.
[38] J. Evans, C.A. Vincent, P.G. Bruce, Polymer 28 (1987) 2324.
[39] N. Tsubokawa, A. Kogure, J. Polym. Sci., Part A: Polym. Chem. 29 (1991) 267.
[40] M. Abboud, M. Turner, E. Duguet, M.J. Fontanille, Mater. Chem. 7 (1997) 8.
[41] C.J. Pouchert (Ed.), The Aldrich Library of FT-IR Spectra, vol. 3, 2nd ed., Aldrich, Milwaukee, WI, 1997.
[42] G.J. Millar, C.H. Rochester, K.C. Waugh, J. Chem. Soc. Faraday Trans. 87 (1991) 2795.
[43] P.P. Chu, M.J. Reddy, J. Power Sources 115 (2003) 288.
[44] Z. Wen, M. Wu, T. Itoh, M. Kubo, Z. Lin, O. Yamamoto, Solid State Ionics 148 (2002) 185.
[45] L. Fan, Z. Dang, C.W. Nan, M. Li, Electrochim. Acta 48 (2002) 205.
[46] P.P. Chu, M.J. Reddy, H.M. Kao, Solid State Ionics 156 (2003) 141.
[47] S. Mitra, A.R. Kulka, Solid State Ionics 154/155 (2002) 37.
[48] J. Przyluski, M. Siekierski, W. Wieczorek, Electrochim. Acta 40 (1995) 2101.
[49] W. Wieczorek, A. Zalewska, M. Siekierski, J. Przyluski, Solid State Ionics 86–88 (1996) 357.
[50] T. Miyamoto, K. Shibayama, J. Appl. Phys. 44 (1973) 5372.
[51] G.B. Appetecchi, G. Dautzenberg, B. Scrosati, J. Electrochem. Soc. 143 (1996) 6.